

Clinical Semantic Intelligence (CSI): Emulating the Cognitive Framework of the Expert Clinician for Comprehensive Oral Disease Diagnosis

Mohammad Mashayekhi^a, Sara Ahmadi Majd^{b,c}, Arian AmirAmjadi^d, Parsa Hosseini^e

^a*Gilan University of Medical Sciences, Rasht, Iran*

^b*University of Göttingen, Göttingen, Germany*

^c*University of Tehran, Tehran, Iran*

^d*Hamadan University of Technology, Hamadan, Iran*

^e*Islamic Azad University, Tehran, Iran*

Abstract

The diagnosis of oral diseases presents a problematic clinical challenge, characterized by a wide spectrum of pathologies with overlapping symptomatology. To address this, we developed Clinical Semantic Intelligence (CSI), a novel artificial intelligence framework that diagnoses 118 different oral diseases by computationally modeling the cognitive processes of an expert clinician. Our core hypothesis is that moving beyond simple pattern matching to emulate expert reasoning is critical to building clinically useful diagnostic aids.

CSI's architecture integrates a fine-tuned multimodal CLIP model with a specialized ChatGLM-6B language model. This system executes a Hierarchical Diagnostic Reasoning Tree (HDRT), a structured framework that distills the systematic, multi-step logic of differential diagnosis. The framework operates in two modes: a Fast Mode for rapid screening and a Standard Mode that leverages the full HDRT for an interactive and in-depth diagnostic workup.

To train and validate our system, we curated a primary dataset of 4,310 images, supplemented by an external hold-out set of 176 images for final validation. A clinically-informed augmentation strategy expanded our training data to over 30,000 image-text pairs. On a 431-image internal test set, CSI's Fast Mode achieved an accuracy of 73.4%, which increased to 89.5% with the HDRT-driven Standard Mode. The performance gain is directly attributable

to the hierarchical reasoning process. Herein, we detail the architectural philosophy, development, and rigorous evaluation of the CSI framework.

Keywords: Oral Disease Diagnosis, Multimodal AI, Clinical Decision Support, Contrastive Language Image Pre-training, Hierarchical Reasoning, ChatGLM-6B

1. Introduction

1.1. *The Clinical Challenge of Oral Diagnosis*

The accurate and timely diagnosis of oral diseases is a cornerstone of patient care, yet it remains a persistent clinical challenge. The vast range of pathologies, from common inflammatory conditions to rare malignancies, frequently present with ambiguous and overlapping clinical features Youngblood et al. (2017); Alrashdan et al. (2016); Scully (2022). This ambiguity can lead to diagnostic uncertainty, resulting in significant delays and misdiagnoses. In fact, studies have shown that up to 14% of patients with oral cancer experience such delays, which is directly correlated with poorer prognoses Scott et al. (2022). The diagnostic problem is further compounded by the relative rarity of certain conditions, such as pemphigus vulgaris or Kaposi sarcoma, which limits the clinical exposure of many practitioners Akpan and Morgan (2021); Cattelan (2020).

1.2. *Our Approach: Emulating the Mind of the Expert Clinician*

Conventional AI approaches to medical imaging often treat diagnosis as a classification task, which does not capture the nuanced, iterative reasoning process of an expert clinician. Our work is based on a different philosophy: To build a truly effective diagnostic aid, AI must emulate the cognitive framework of a specialist. To that end, we developed **CSI (Clinical Semantic Intelligence)**, a system designed to "think" like an oral pathologist.

Our design philosophy is rooted in modeling two key aspects of expert cognition.

1. **Dual-Speed Reasoning:** Specialists fluidly switch between rapid, intuitive pattern recognition for classic cases and a slower, more deliberate analytical process for ambiguous presentations. CSI mirrors this with its *Fast Mode* and *Standard Mode*.

2. **Hierarchical, Reductive Logic:** For a complex case, an expert does not simply guess. They systematically narrow the possibilities through a structured inquiry, a process that we computationally model with our *Hierarchical Diagnostic Reasoning Tree (HDRT)*.

By integrating multimodal data analysis with this expert-emulating reasoning structure, CSI aims to provide a diagnostic tool that is not only accurate but also transparent and clinically intuitive.

1.3. Objectives

The primary objective of this study was to develop and rigorously validate an AI model capable of accurately diagnosing a comprehensive range of 118 oral diseases. Our central hypothesis was that by computationally modeling the hierarchical reasoning process of clinicians, we could achieve a significant improvement in diagnostic precision over standard, non-interactive classification methods. We sought to build a system that could serve as a reliable decision support tool, with the ultimate goal of reducing diagnostic errors and improving patient oral health.

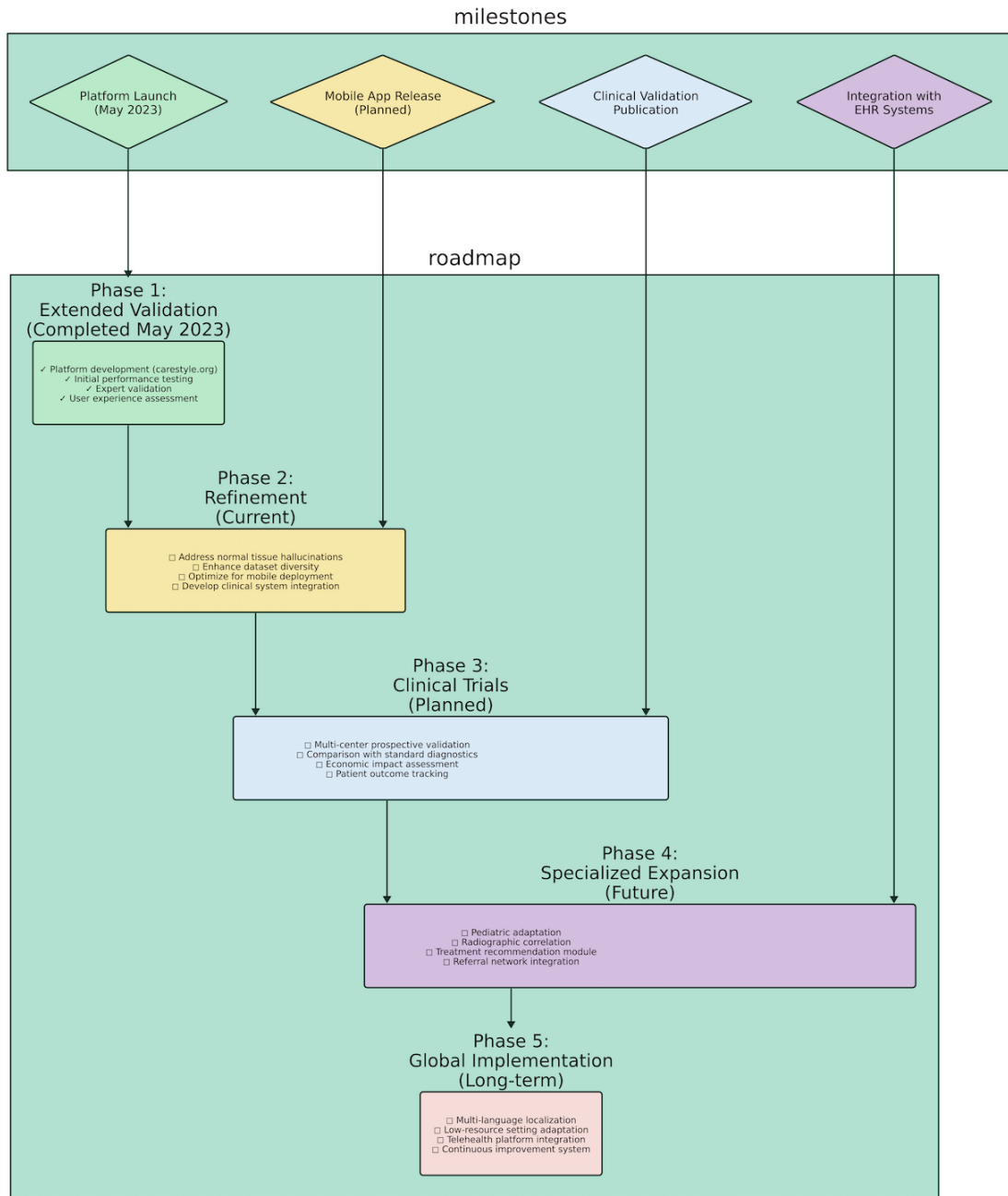


Figure 1: Project timeline from April 2023 to September 2023, depicting the major development milestones of the CSI framework.

2. Literature Review and Related Work

The challenge of differential diagnosis in oral pathology is well documented Neville et al. (2015). Although AI in dentistry has shown promise, particularly through the application of CNNs to radiographic analysis Lee et al. (2018), most systems address narrow tasks and lack the capacity for comprehensive and interactive differential diagnosis. The advent of powerful multimodal models like CLIP has shown the potential of aligning visual and textual data for a deeper semantic understanding Radford et al. (2021). Currently, the integration of large language models into interactive systems offers a pathway to resolve clinical ambiguity through discussions Li et al. (2020). Our work builds on these advances but addresses a critical gap by combining them with the principles of hierarchical decision modeling Quinlan (1986), a concept long established in medical informatics. CSI’s novelty lies in synthesizing these three parts, multimodal learning, interactive dialogue, and hierarchical reasoning, into a single cohesive framework that emulates the full arc of expert clinical evaluation.

3. Dataset and Methods

3.1. Dataset Curation and Partitioning

To build a robust training corpus, we curated a primary dataset of 4,310 high-quality clinical images. Archival images (dating from 2021 to 2023) were curated and augmented between April and September 2023, sourced from authoritative medical textbooks, collaborations with multiple dental clinics, and direct contributions from clinical practices (see Acknowledgments). To establish a reliable ground truth for evaluation, all images in our test set were verified on the basis of biopsy results, where applicable. The primary data set was partitioned for the development of the model, and a separate external validation set of 176 images was reserved for the final and unbiased comparison (Table 1).

Table 1: Partitioning of the primary and external validation datasets.

Partition	Percentage	Image Count	Purpose
Training	70%	3,017	Model training
Validation	20%	862	Hyperparam. tuning
Internal Test	10%	431	Internal evaluations
External Validation	N/A	176	Unbiased benchmark on complex cases

3.2. Data Augmentation Strategy

To mitigate class imbalance inherent in clinical data, we developed a clinically-grounded augmentation strategy that expanded our dataset to approximately 30,000 image-text pairs. This involved both pathology-preserving image transformations and text-based augmentation to create diverse yet realistic clinical scenarios. To systematically balance the dataset, we employed a distribution-aware sampling formula:

$$\text{Augmentation Factor} = \log(b) + a \times \left(1 - \frac{N_{\text{initial}}}{N_{\text{max}}}\right) \quad (1)$$

N_{initial} is the image count for a given disease, and N_{max} is the count for the most common disease. Based on empirical validation, where different settings were evaluated on a held-out portion of the training set to identify a configuration that provided a satisfactory balance, as confirmed by expert review, we set the tuning parameters at $a = 10$ and $b = 2$.

3.3. Diagnostic Zones and The Expert-Corrected Atlas

Following training, we used t-SNE to visualize the model’s learned embedding space for all 118 diseases. This visualization, which we termed the **Expert-Corrected Diagnostic Atlas** (Figure 2), revealed how the model organizes diseases based on their semantic and visual features. From this analysis, and validated by a panel of five oral pathologists, we defined three diagnostic zones that categorize diseases by their intrinsic diagnostic difficulty:

- **Zone 3 (Routine):** Conditions with pathognomonic features.
- **Zone 2 (Intermediate):** Conditions with significant overlap of characteristics requiring clinical context.

- **Zone 1 (Complex):** Rare or diagnostically challenging conditions that often require biopsy.

The internal test set (N = 431) consisted of 241 images of Zone 3 (55.9%), 153 images of Zone 2 (35.5%), and 37 images of Zone 1 (8.6%).

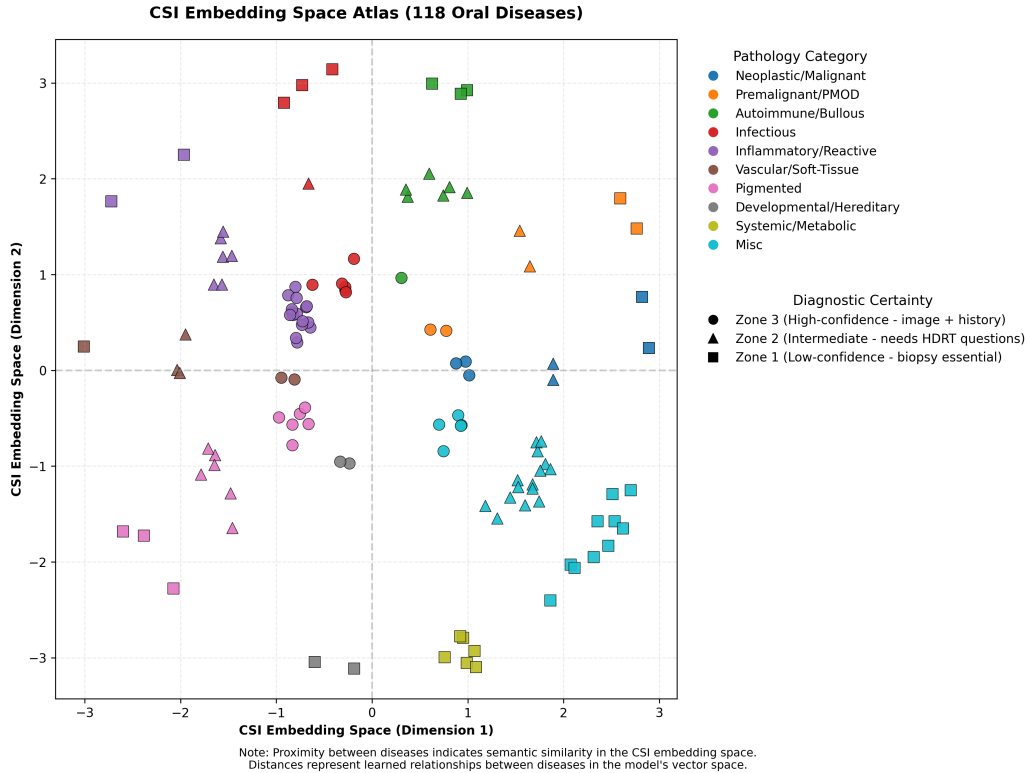


Figure 2: The CSI Embedding Space Atlas, mapping 118 oral diseases. Colors represent pathology families, shapes represent diagnostic zones (circle: Zone 3, triangle: Zone 2, square: Zone 1), and distance from the center correlates with diagnostic certainty.

3.4. Model Architecture

The architectural philosophy of CSI is rooted in an additive approach, enhancing powerful foundation models with specialized clinical knowledge without compromising their general capabilities.

3.4.1. The Multimodal Fusion Model: Creating a Clinical Gestalt

The diagnostic process begins with a fusion model that integrates visual and textual input to create a unified semantic representation: a compu-

tational analog of a clinician’s initial ”gestalt.” We used a CLIP ViT-H/14 architecture, fine-tuned with the Wise-FT method Wortsman et al. (2022) to prevent catastrophic forgetting. The image and text features are projected into a common embedding space and fused into a single 1024-dimensional vector that encapsulates the case.

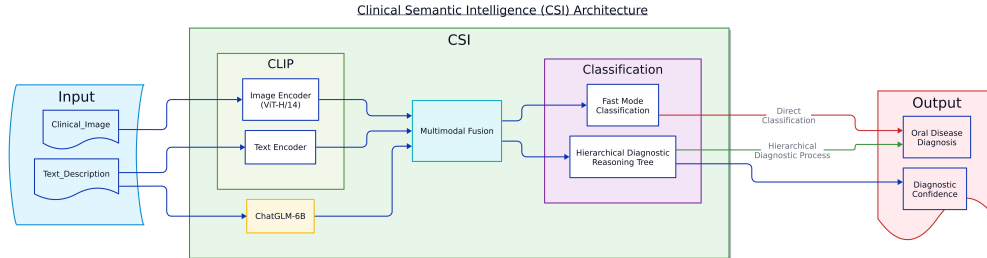


Figure 3: High-level overview of the CSI model architecture. It depicts the initial fusion of multimodal inputs to form a semantic representation, which is then processed by the dual-capability ChatGLM-6B model executing the HDRT.

3.4.2. ChatGLM-6B: A Dual-Capability Language Engine

Our central innovation was to endow a single ChatGLM-6B model with two distinct capabilities through sequential supervised fine-tuning (SFT) on a 40 million token dental corpus.

1. **First SFT (Clinical Communicator and Router):** This phase trained the model to be an intelligent clinical interface, capable of managing conversation and routing queries appropriately.
2. **Second SFT (HDRT Executor):** This phase trained the same model to accept the semantic vector of the fusion model and execute the structured reasoning of the HDRT.

3.4.3. The Hierarchical Diagnostic Reasoning Tree (HDRT)

The HDRT is the computational core of CSI’s Standard Mode. It models the systematic, reductive reasoning of an expert by proceeding through six distinct levels of analysis. It is crucial to distinguish the six HDRT *levels*, which describe the sequential steps in the reasoning process, from the three diagnostic *zones*, which categorize the diseases themselves by difficulty. To

handle uncertainty, a confidence threshold gating mechanism asks the user for more information if the top two diagnoses have similar probabilities, thereby simulating a clinical dialogue.

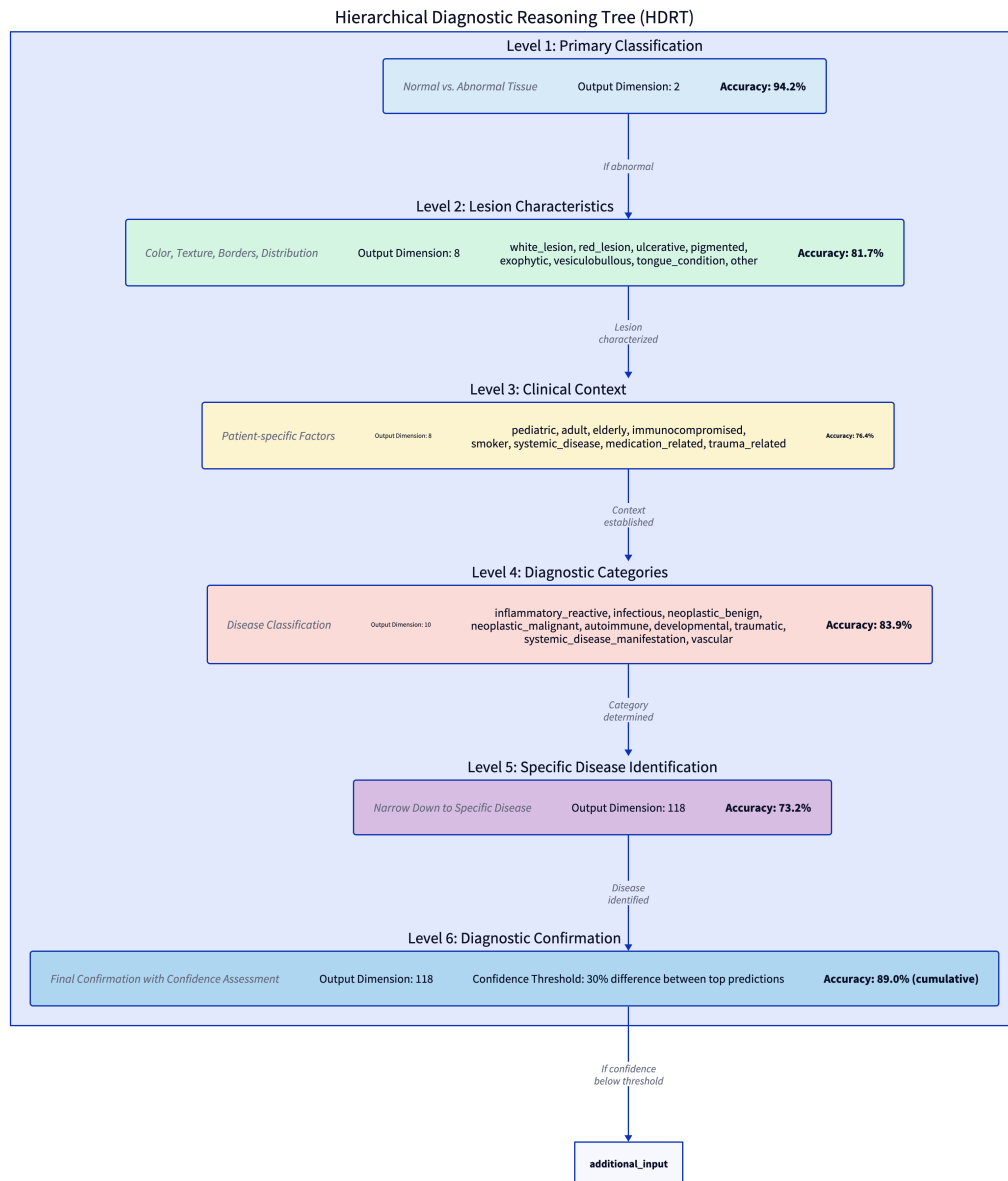


Figure 4: Conceptual diagram of the Hierarchical Diagnostic Reasoning Tree (HDRT). This figure illustrates the high-level flow of the six-level clinical reasoning process. The specific operations and logic at each level are detailed in Appendix B.

4. Results

4.1. Performance on the Internal Test Set

We first evaluated CSI’s performance on the 431-image internal test set. The results, shown in Table 2, highlight the substantial performance gain provided by the HDRT framework. For comparison, GPT-4 was evaluated in a non-interactive, zero-shot setting.

Table 2: Zone-specific accuracy (%) on the internal test set (N=431).

Zone	Test Images	Fast Mode	Standard Mode	GPT-4
Zone 3 (Routine)	241	85.4	94.3	79.4
Zone 2 (Intermediate)	153	63.7	89.5	60.2
Zone 1 (Complex)	37	35.8	58.1	38.7
Overall	431	73.4	89.5	69.1

* Overall accuracy is the weighted average calculated based on the number of test images in each diagnostic zone.

The greatest performance differential was observed in Zone 2, where HDRT improved accuracy by 25.8 percentage points, underscoring the value of contextual reasoning for diseases with overlapping features.

4.2. Performance on the External Validation Dataset

To assess the model’s real-world generalization, we curated a challenging external validation set of 176 cases. This set was intentionally skewed towards more difficult cases, with a distribution of: Zone 1 (N=15, 8.5%), Zone 2 (N=75, 42.6%), and Zone 3 (N=86, 48.9%).

Table 3: Comparative performance (%) on the complex external validation set (N=176).

Metric	Fast Mode	Standard Mode	GPT-4
Zone 3 Accuracy	77.9	90.7	68.6
Zone 2 Accuracy	56.0	85.3	57.3
Zone 1 Accuracy	33.3	53.3	13.3
Overall Accuracy	64.8	85.2	58.5

* Overall accuracy is the weighted average based on the zone distribution of this external set.

Even on this difficult, unseen dataset, CSI’s Standard Mode demonstrated robust performance (85.2%), maintaining a significant advantage over both its non-interactive counterpart and the generalist GPT-4 model.

5. Discussion

5.1. *The Value of Emulating Clinical Reasoning*

The central contribution of this work is a paradigm shift from conventional AI classification to the emulation of domain-specific diagnostic reasoning. By computationally modeling the hierarchical logic of an expert clinician, CSI achieves a "cognitive fidelity" that allows it to systematically navigate diagnostic uncertainty. This is not merely an academic exercise; it directly addresses the clinical challenge of differentiating pathologies with overlapping features. The superior performance of the Standard Mode over the Fast Mode provides clear evidence that, for complex medical tasks, the reasoning process itself is as important as the final classification.

5.2. *Clinical Implications and Comparative Performance*

The CSI framework has significant potential as both a clinical decision support tool and an educational platform. For practitioners in underserved areas, it can provide access to specialist-level reasoning. For trainees, the transparent step-by-step diagnostic pathways can serve as a powerful learning aid. Our findings indicate a clear performance advantage for the hierarchical specialized approach of CSI compared to the zero-shot capabilities of a generalist model like GPT-4 (85.2% vs. 58.5% on the external set).

However, a critical caveat is that this represents an asymmetric benchmark. We compared our interactive, multi-turn Standard Mode against a single-turn evaluation of GPT-4. This design effectively highlights the value added by the HDRT’s interactive framework, but a direct comparison of conversational diagnostic capabilities would require a symmetric evaluation where the baseline model is also engaged in a structured dialogue. This benchmark was outside the scope of this study, but it represents a critical direction for future work.

5.3. *Limitations and Future Directions*

This study has several limitations. Our model can occasionally misclassify normal anatomical variants. Although our data set is extensive, it may not capture the full spectrum of global diversity in disease presentation.

Furthermore, the performance of the interactive Standard Mode is inherently dependent on the quality of user-provided information. Future work will focus on expanding the dataset, optimizing the model for deployment in resource-limited settings, and enhancing the natural language interface. Ultimately, large-scale, multicenter clinical trials are required to definitively validate the real-world efficacy of the CSI framework.

6. Conclusion

Clinical Semantic Intelligence (CSI) provides a robust framework for AI-assisted oral diagnosis, distinguished by its foundational philosophy of emulating expert clinical reasoning. By integrating multimodal analysis with a hierarchical interactive diagnostic process, CSI successfully diagnoses a comprehensive range of 118 oral diseases with a high degree of precision and interpretability. Our results, particularly the 85.2% accuracy achieved on a challenging external validation set, confirm that for specialized medical domains, an architecture that models the expert’s cognitive process significantly outperforms generic, non-interactive approaches. Although further validation is necessary, the CSI framework represents a promising step toward developing AI systems that function not as black-box classifiers but as transparent and collaborative partners in the complex art of clinical diagnosis.

Acknowledgements

The authors thank Dr. Babak Mashayekhi for his invaluable contribution of clinical images from his practice, which were essential for the curation of our datasets. The authors also acknowledge the support of the Gilan University of Medical Sciences in facilitating this research.

Appendix A: Comprehensive List of Oral Diseases Detectable by CSI

1. Pemphigus Vulgaris
2. Lichenoid Contact Reaction
3. Geographic Tongue
4. Erythema Multiforme
5. Acquired Hemangioma
6. Verruciform Xanthoma
7. Hemangioma
8. Palatal Keratosis Associated with Reverse Smoking
9. Denture Stomatitis
10. Hereditary Benign Intraepithelial Dyskeratosis
11. Necrotizing Ulcerative Gingivitis
12. Squamous Cell Carcinoma
13. Capillary Hemangioma
14. Hypoadrenocorticism
15. Recurrent Herpes Stomatitis
16. Lichenoid Reaction
17. Submucous Fibrosis
18. Cytomegalovirus-Associated Ulceration
19. Non-Hodgkin Lymphoma
20. Verruca Vulgaris
21. Schwannoma
22. Lymphangioma
23. Plasma Cell Stomatitis

24. Pyogenic Granuloma
25. Inflammation-Associated Hyperpigmentation
26. Traumatic Ulcer
27. Neurofibroma
28. Smoker's Melanosis
29. Angular Cheilitis
30. Erythematous Lichen Planus
31. Irritation Fibroma
32. Physiologic Pigmentation
33. Actinic Cheilitis
34. Varicosities
35. Mucocele and Ranula
36. Herpangina
37. Hyperthyroidism
38. Pulp Polyp
39. Melanotic Macule
40. Candidal Leukoplakia
41. Cushing's Disease
42. Nicotinic Stomatitis
43. Superficial Oral Burn
44. Graft vs. Host Disease
45. Epidermolysis Bullosa
46. Lupus Erythematosus
47. Peripheral Ossifying Fibroma
48. Oral Leukoplakia

49. Peripheral Giant Cell Granuloma
50. Adenoid Cystic Carcinoma
51. Drug-Induced Lichenoid Reaction
52. Chemotherapy-Related Ulcers
53. Erythroplakia
54. Squamous Papilloma
55. Giant Cell Fibroma
56. Oral Lichen Planus
57. Malignant Melanoma
58. Verrucous Hyperplasia
59. Pregnancy Tumor
60. Eosinophilic Ulcer
61. Vascular Malformation
62. Vitamin B12 Deficiency
63. Medicinal Metal-Induced Pigmentation
64. Epulis Granulomatosum
65. Smokeless Tobacco Keratosis
66. Oral Hypersensitivity Reactions
67. White Sponge Nevus
68. Frictional Keratosis
69. Hematoma-Echymosis-Petechia-Purpura
70. Keratoacanthoma
71. Laugier-Hunziker Pigmentation
72. Lipoma
73. Morsicatio

74. Hereditary Hemorrhagic Telangiectasia
75. Oral Hairy Leukoplakia
76. Bullous Pemphigoid
77. Epulis Fissuratum
78. Parulis
79. Freckle-Ephelis
80. Verrucous Carcinoma
81. Peutz-Jeghers Syndrome
82. Melanocytic Nevus
83. Leaflike Fibroma
84. Ulcerative Squamous Cell Carcinoma
85. Xeroderma Pigmentosum
86. Amalgam Tattoo
87. Vesiculobullous Diseases
88. Necrotizing Sialometaplasia
89. Recurrent Aphthous Stomatitis
90. Oral Melanoacanthoma
91. Graft-versus-Host Disease
92. Reticular Lichen Planus
93. Deep Fungal Ulceration
94. Inflammatory Papillary Hyperplasia
95. Kaposi Sarcoma
96. Behçet's Disease
97. Dyskeratosis Congenita
98. Median Rhomboid Glossitis

99. Erythematous Candidiasis
100. Tuberculous Ulcer
101. Mucous Membrane Pemphigoid
102. Multifocal Epithelial Hyperplasia
103. Chancre or Syphilitic Ulceration
104. Leukoedema
105. Shingles
106. Café au Lait Pigmentation
107. Cheilitis Glandularis
108. Melasma
109. Primary Herpetic Gingivostomatitis
110. Cyclic Neutropenia
111. Chronic Mucocutaneous Candidiasis
112. Angiosarcoma
113. Hairy Tongue
114. Sustained Traumatic Ulcer
115. Drug-Induced Melanosis
116. Proliferative Verrucous Leukoplakia
117. Pseudomembranous Candidiasis
118. HIV-Associated Pigmentation

Appendix B: HDRT Framework Technical Details

B.1 Multimodal Integration Details

- **Projection Layers:**

1. CLIP Image Projection: Linear(1280→1024)
2. CLIP Text Projection: Linear(1024→1024)
3. GLM Projection: Linear(4096→1024)

- **CLIP Fusion:** Concatenate image & text features, reduce dimension (2048→1024).

- **Multimodal Fusion:** Concatenate CLIP-fused & GLM features (2048→1024).

B.2 HDRT Level-Specific Dimensions

- **Level 1:** Primary classification (2 outputs: normal/abnormal).

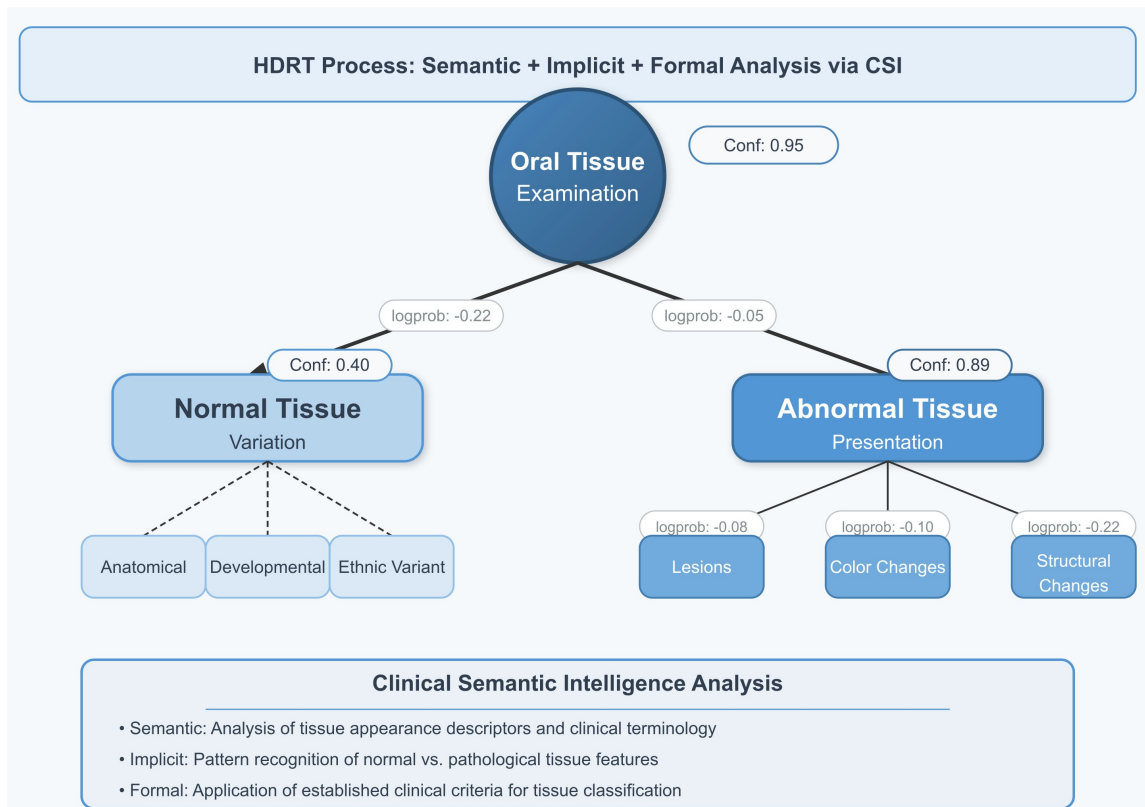


Figure .5: Primary Classification: Initial assessment of oral tissue with confidence scoring

- **Level 2:** Lesion characteristics (8 outputs by color/texture).

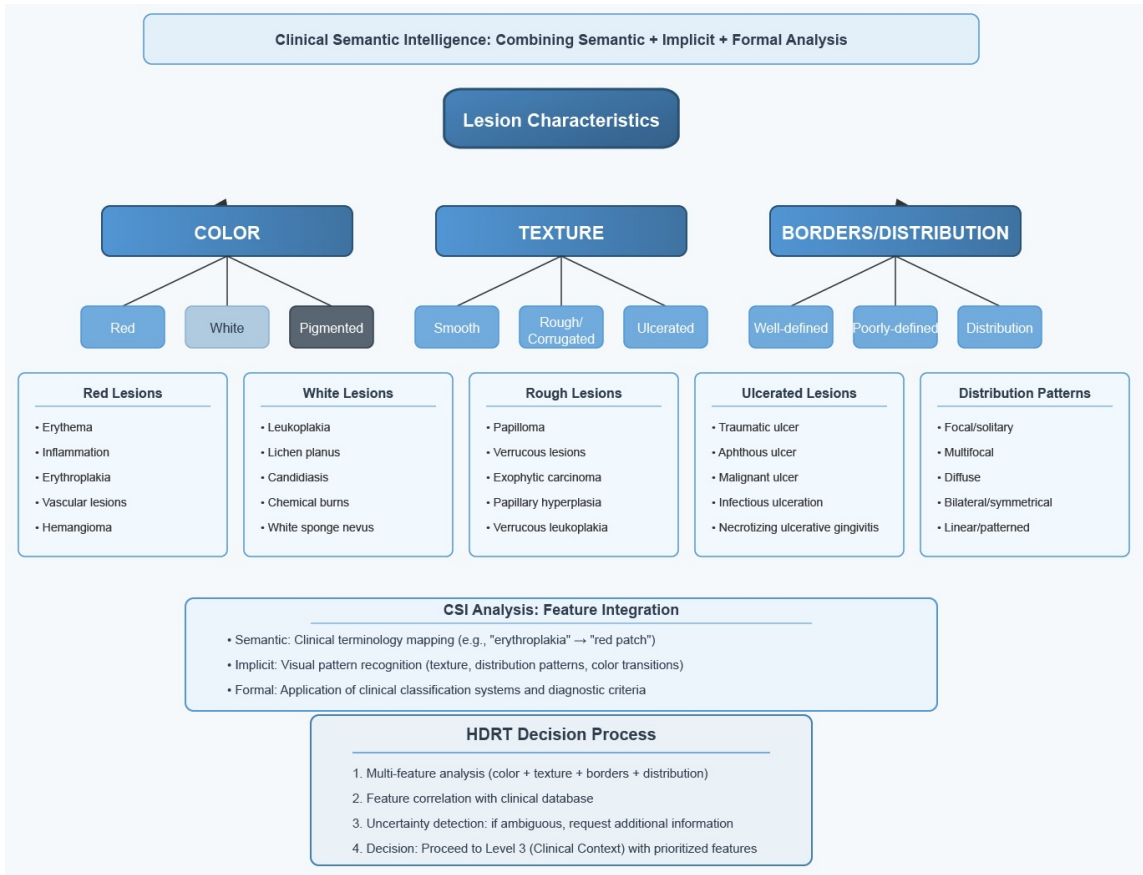


Figure .6: Lesion Characteristics: Assessment of visible abnormalities with CSI analysis

- **Level 3: Clinical context** (8 outputs according to demographic/ risk).

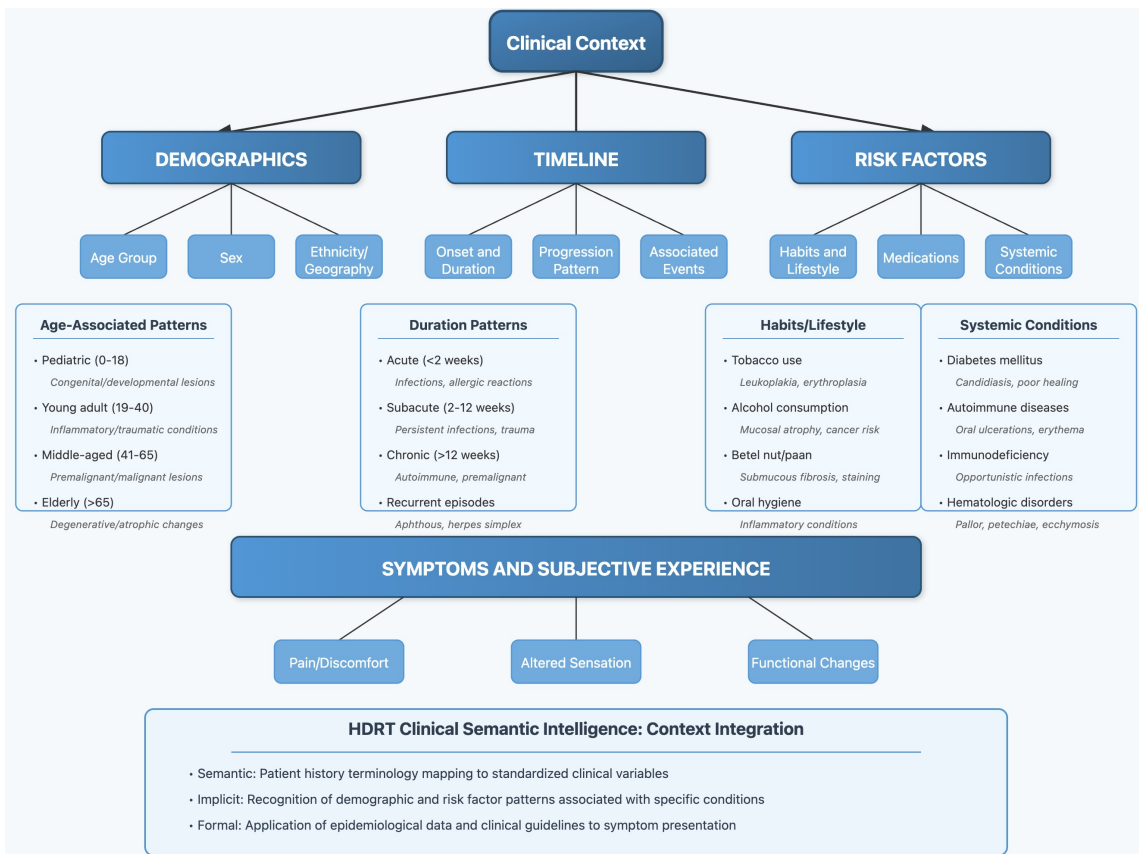


Figure .7: Clinical Context: Patient-specific factors that influence diagnostic assessment.

- **Level 4:** Diagnostic categories (10 outputs: inflammatory, neoplastic, etc.).

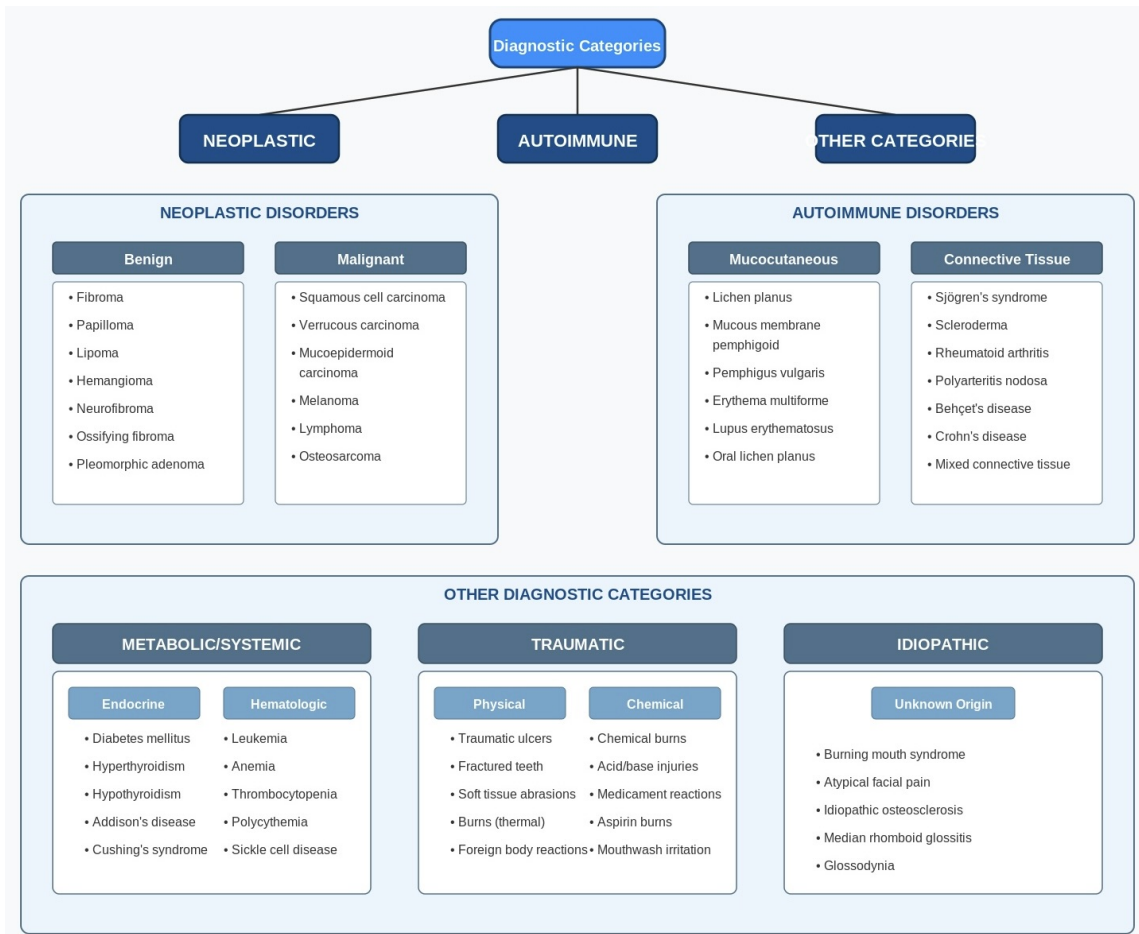


Figure .8: Diagnostic Categories: Neoplastic, autoimmune, and additional groupings.

- **Level 5: Disease identification** (118 possible diseases).

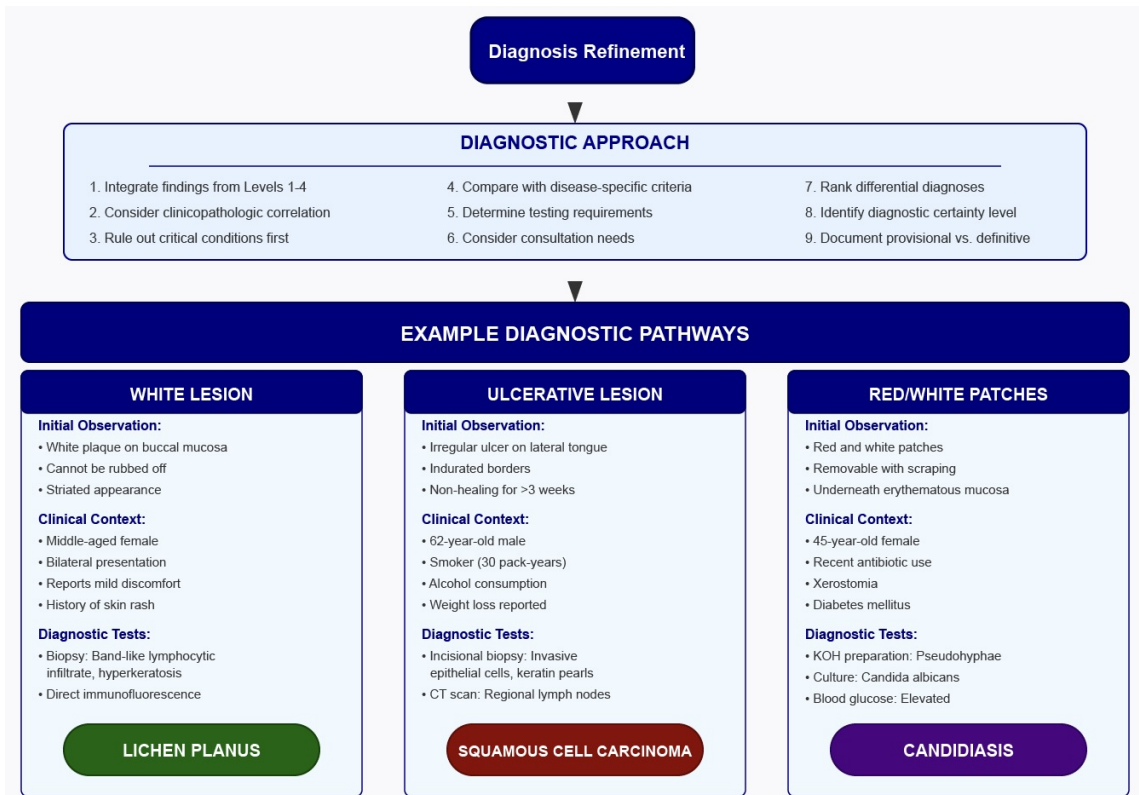


Figure .9: Specific Disease Identification: Narrowing down to a specific diagnosis based on combined evidence (covering 118 possible conditions).

- **Level 6:** Diagnostic confirmation (118 final probabilities).

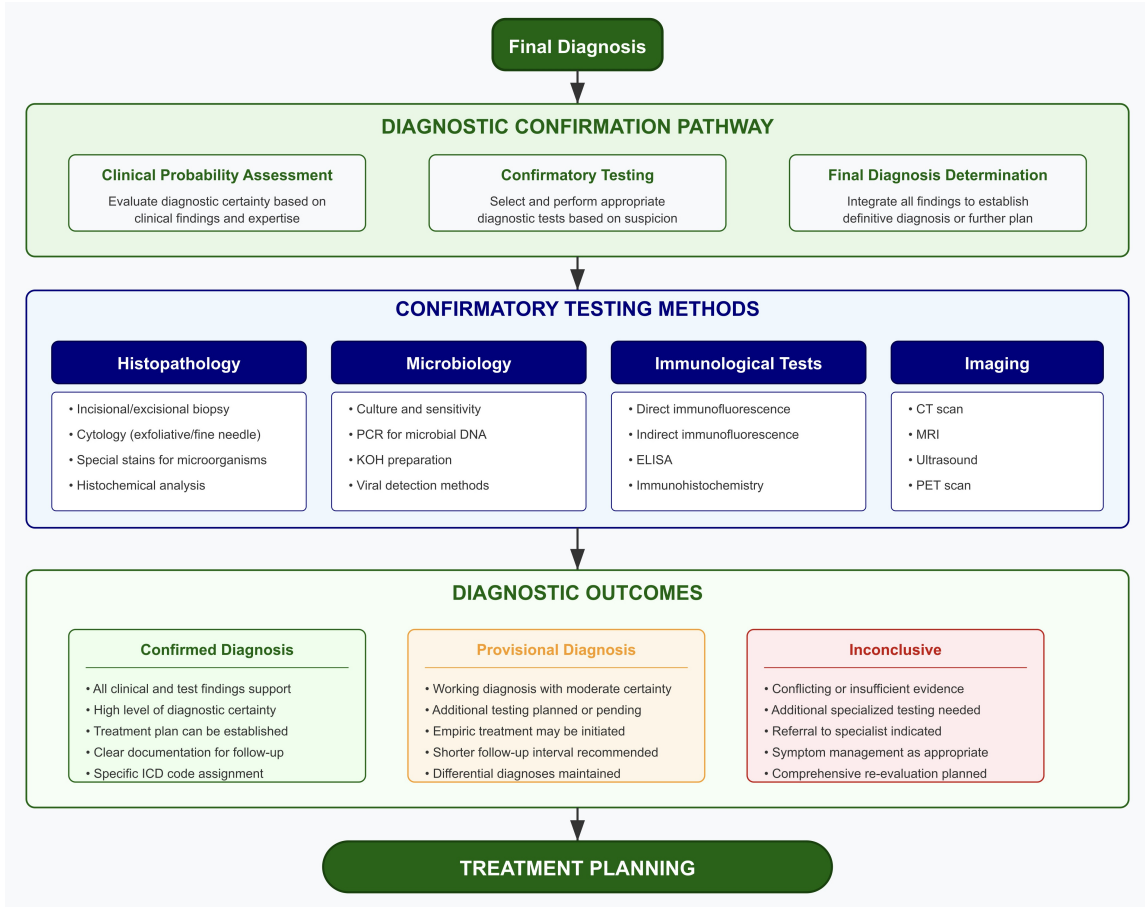


Figure .10: Diagnostic Confirmation: Final assessment, confirmatory testing, and treatment planning.

B.3 Confidence-Threshold Gating Implementation

When the difference between the logarithmic probabilities of the top two ranked diagnoses is below a threshold of 0.3, the system flags the uncertainty and is prompted to request additional clarification input from the user.

Appendix C: CSI Output Examples

C.1 Fast Mode Output Example

- **Primary Diagnosis:** Oral Lichen Planus (78.5% confidence)
- **Differential Diagnosis:**
 - Lichenoid Reaction (12.3%)
 - Leukoplakia (5.7%)
 - Candidal Leukoplakia (2.1%)

C.2 Standard Mode Output Example

- **Diagnostic Path:** Abnormal → White Lesion → Adult → Inflammatory/Reactive → Oral Lichen Planus
- **Final Diagnosis:** Oral Lichen Planus (85.3% confidence, high certainty)
- **Differential Diagnosis:** 1. Lichenoid reaction (8.1%), 2. Leukoplakia (3.4%)
- **Diagnostic Conversation:**
 1. *Q1:* What are the main visual characteristics of this lesion?
 2. *A1:* White reticular pattern in the buccal mucosa, bilateral presentation.
 3. *Q2:* Any significant history of medications?
 4. *A2:* No recent changes, no known triggers.

C.3 ChatGLM-Enhanced Interactive Response Example

User Query: "What is the difference between oral lichen planus and that lichen-like reaction?"

CSI Response:

Based on the diagnostic assessment, several key differences can be highlighted between Oral Lichen Planus and a Lichenoid Reaction:

1. Bilateral, reticular lesions with characteristic Wickham's striae strongly favor Oral Lichen Planus, whereas Lichenoid Reactions tend to be more localized or unilateral.

2. The absence of known triggers, such as new medications or dental materials, reduces the likelihood of a lichenoid reaction.
3. A mild burning sensation is more typical for Oral Lichen Planus.

Based on this reasoning, confidence is 85.3% for Oral Lichen Planus versus 8.1% for a Lichenoid Reaction. A biopsy may be recommended for definitive differentiation.

References

- Akpan, A., & Morgan, R. (2021). Pemphigus vulgaris: A new approach to diagnosis. *British Journal of Oral and Maxillofacial Surgery*, 59, 456–462.
- Alrashdan, M. S., Cirillo, N., & McCullough, M. (2016). Oral lichen planus: a literature review and update. *Archives of Dermatological Research*, 308(8), 539–551.
- American Cancer Society. (2024). Survival rates for oral cavity and oropharyngeal cancer. Available at: <https://www.cancer.org/cancer/types/oral-cavity-and-oropharyngeal-cancer/detection-diagnosis-staging/survival-rates.html>.
- Cattelan, A. M. (2020). HIV-related Kaposi's sarcoma in the era of HAART. *European Review for Medical and Pharmacological Sciences*, 24(8), 5072–5081.
- Centers for Disease Control and Prevention. (2024). Oral health equity. Available at: <https://www.cdc.gov/oral-health/health-equity/index.html>.
- Emami, E., & Kisely, S. (2021). A systematic review of the effectiveness of educational interventions to reduce misdiagnosis in dentistry. *International Journal of Dentistry*, 9(1), 56–62.
- GBD 2021 Oral Conditions Collaborators. (2022). Trends in global, regional, and national burden of oral conditions, 1990–2021: a systematic analysis for the Global Burden of Disease Study 2021. *The Lancet*, 400(10352), 1549–1568.
- Lee, J.-H., et al. (2018). Deep learning in medical imaging: general overview. *Korean Journal of Radiology*, 19(4), 927–937.
- Li, Y., et al. (2020). Clinical dialogue system using multi-turn hierarchical pre-training. *Proceedings of the 58th Annual Meeting of the Association for Computational Linguistics*, 9018–9028.
- Nedu, M. E., Zeola, L. F., Giraldo, F. G., et al. (2021). Interobserver variability in the clinical diagnosis of oral potentially malignant disorders. *Oral Surgery, Oral Medicine, Oral Pathology and Oral Radiology*, 131(3), 296–304.

- Neville, B. W., et al. (2015). *Oral and Maxillofacial Pathology* (4th ed.). Elsevier.
- Petersen, P. E., et al. (2005). The global burden of oral diseases and risks to oral health. *Bulletin of the World Health Organization*, 83(9), 661–669.
- Quinlan, J. R. (1986). Induction of decision trees. *Machine Learning*, 1(1), 81–106.
- Radford, A. et al. (2021). Learning transferable visual models from natural language supervision. *Proceedings of the 38th International Conference on Machine Learning*, PMLR 139:8748–8763.
- Scott, S. E., et al. (2022). Professional delays in the diagnosis of oral cancer: A case series. *British Dental Journal*, 233(10), 829–834.
- Scully, C. (2022). Aphthous ulceration: new perspectives on pathogenesis and management. *Current Oral Health Reports*, 9(3), 114–122.
- Varela-Centelles, P., et al. (2021). Diagnostic delay in oral cancer: A systematic review. *Medicina Oral, Patología Oral y Cirugía Bucal*, 26(6), e750–e759.
- World Health Organization. (2022). Global Oral Health Status Report: Towards universal health coverage for oral health by 2030. Geneva: WHO.
- Wortsman, M., et al. (2022). Model soups: Averaging weights of multiple fine-tuned models improves accuracy without increasing inference time. *arXiv preprint arXiv:2203.05482*.
- Youngblood, B., Brierley, D. J., Freedman, M., et al. (2017). Pigmented lesions of the oral cavity. *Atlas of the Oral and Maxillofacial Surgery Clinics*, 25(1), 39–47.